Hybrid Ionization Source Combining Nano-electrospray and Dielectric Barrier Discharge Ionization for Simultaneous Detection of Polar and Non-polar Compounds in Single Cells

Hybrid Ionization Source Combining Nano-electrospray and Dielectric Barrier Discharge Ionization for Simultaneous Detection of Polar and Non-polar Compounds in Single Cells

Qinlei Liu,[a] Jiayi Lan,[a] Ri Wu,[a] Alina Begley,[a] Wenjie Ge,[b] Renato Zenobi*[a]

[a]Department of Chemistry and Applied Biosciences, ETH Zurich, Zurich CH-8093, Switzerland

[b]Department of Biology, ETH Zurich, CH-8093 Zurich, Switzerland

Corresponding Author

Renato Zenobi

E-mail: zenobi@org.chem.ethz.ch

ABSTRACT

Single-cell metabolomics is expected to deliver fast and dynamic information on cell function, therefore, it requires rapid analysis of a wide variety of very small quantities of metabolites in living cells. In this work, a hybrid ionization source that combines nano-electrospray ionization (nanoESI) and dielectric barrier discharge ionization (DBDI) is proposed for single-cell analysis. A capillary with a 1 µm i.d. tip was inserted into cells for sampling, and then directly used as the nanoESI source for ionization of polar metabolites. In addition, a DBDI source was employed as post-ionization source to improve the ionization of apolar metabolites in cells that are not easily ionized by ESI. By increasing the voltage of the DBDI source from 0 to 3.2 kV, the classes of detected metabolites can be shifted from mostly polar to both polar and apolar to mainly apolar. Plant cells (onion) and human cells (PANC-1) were investigated in this study. After optimization, 50 compounds in onion cells and 40 compounds in PANC-1 cells were observed in ESI mode (3.5 kV), and an additional 49

compounds in onion cells and 73 compounds in PANC-1 cells were detected in ESI (3.5 kV)-DBDI (2.6 kV) hybrid mode. This hybrid ionization source improves the coverage, ionization efficiency, and limit of detection of metabolites with different polarities, and could potentially contribute to the fast-growing field of single-cell metabolomics.

INTRODUCTION

Single-cell metabolic analysis provides useful information about cellular heterogeneity.[1-3] However, single-cell metabolomics is very challenging due to the low abundance and diverse structure of intracellular metabolites.

Mass spectrometry is a label-free analytical technique with high sensitivity, good selectivity, and fast response. It can simultaneously detect multiple low molecular weight metabolites in a cell and has been widely used for single-cell metabolomics.[4-6] The ionization method is crucial, as it determines the coverage and limit of detection (LOD) of the metabolome. Mass spectrometry based single-cell metabolomics mainly relies on secondary ion mass spectrometry (SIMS),[3,7,8] matrix-assisted laser desorption/ionization mass spectrometry (MALDI-MS),[9,10] and nano-electrospray ionization mass spectrometry (nanoESI-MS).[2,11] SIMS has a high spatial resolution and can be used for subcellular analysis, but many fragments are usually generated during the ionization process. Although the spatial resolution of MALDI is far less than that of SIMS, MALDI is a soft ionization source that can detect many types of compounds with relatively high sensitivity. MALDI and SIMS have many applications in the area of single-cell imaging.[8,12,13] ESI-based methods can be used for sampling and ionization of metabolites in living cells. Pioneering work in this area has been done by Masujima and co-workers.[14-16] They developed a “live single-cell MS” (LSC-MS) method and applied it to analyze metabolites in mouse embryonic fibroblasts cells,[16] human-derived

circulating tumor cells (CTCs),[14] and plant cells.[15] Vertes and coworkers have demonstrated the efficient use of capillary microsampling combined with ESI and ion mobility separation (IMS) followed by MS for the analysis of single plant and animal cells.[17-19] Single cell metabolite analysis by laser ablation ESI (LAESI) MS was also practiced by the same group,[20,21] and recently, they used it for single-cell high-throughput analysis.[22] Nemes and coworkers combined capillary electrophoresis (CE) and ESI-MS for single-cell analysis.[23-25] More recently, they enabled in-vivo single-cell proteomics and metabolomics in South African clawed frog embryos via CE-ESI-MS.[26] Both of these groups used probe sampling and ESI ionization methods to study single cells. Each single-cell ionization method has its own advantages. For example, nanoESI is suitable for the ionization of polar metabolites, but it less suitable for ionizing non-polar metabolites, due to its ionization mechanism.

We reasoned that different ionization methods can complement each other, which should be beneficial for the study of single-cell metabolomics. For example, dielectric barrier discharge ionization (DBDI) source is a sensitive, efficient, and cheap low-temperature plasma source, which is based on completely different ionization processes than ESI.[27,28] The plasma contains many reactive species, including electrons, ions, neutral atoms, excited states, radicals, and photons.[29] Reactive species in the plasma determine the ionization reactions and product ions.[28,30,31] Some reactive species (e.g., $N_2^{+\bullet}$, $O_2^{+\bullet}$, N_2*) will lead to charging of non-polar compounds through charge transfer, electron impact or Penning ionization processes, while other reactive species (e.g., $(H_2O)_nH^+$) ionize polar compounds via protonation. The applied voltage is a crucial parameter that influences the ionization efficiency and selectivity of the generated product ions. By increasing the plasma voltage, the energy and the number of electrons will increase.[32] A high applied voltages will thus increase the ionization efficiency.[33] In addition, DBDI can be operated with dopants to boost the ion

yield of specific analytes.[34] Our group has developed a small, soft, and practical DBDI source with high ion transmission efficiency and has used it for single-cell metabolism analysis.[35] We have proven that DBDI-MS can detect multiple metabolites at the single-cell level and distinguish different cell types based on the detected metabolites information.

Possible strategies to improve the ionization efficiency of non-polar metabolites and expand the detection range of metabolites in single cells are to develop alternative ionization sources, post-ionization sources, or versatile hybrid ionization sources for single-cell metabolomics. Hybrid ionization sources have been used in the past, although only on the bulk level, never in the context of the analysis of non-polar metabolites in single cells. For example, Shiea and co-workers introduced a combination of ESI with atmospheric pressure chemical ionization to post-ionize neutrals produced by laser desorption and thermal desorption. Both polar and non-polar analytes were observed.[36] Another example is the use of matrix-assisted laser desorption electrospray ionization (MALDESI) for imaging applications, which was pioneered by Muddiman and co-workers.[37,38] They combined the benefits of MALDI and ESI post-ionization to increase the ion yield. The Franzke group also reported that DBDI can increase the signal intensity of lysine that has been ionized by ESI.[39] The general concept is to use a post-ionization scheme to boost the ion yield, and we propose that it would also be advantageous to ionize non-polar metabolites and metabolites that exhibit low ionization yield. Therefore, we hypothesized that combining ESI and DBDI will enlarge the range of metabolites that can be covered and lower the LOD, which is crucial for single-cell metabolomics.

In this study, we introduce a hybrid nanoESI-DBDI source for single-cell analysis, which has two modes: an "ESI mode" and a "hybrid mode" to detect intracellular metabolites with different polarities. As a proof of principle, a glass capillary with a tip diameter of 1 µm was

inserted into a cell for sucking in cell contents (Figure 1a), and then the cellular metabolites were ionized by the hybrid nanoESI-DBDI source (Figure 1b), where the nanoESI primarily ionizes polar metabolites, followed by a DBDI source as a post-ionization source to ionize less polar, non-polar metabolites and metabolites with low ESI ionization yield. We were able to demonstrate detection of metabolites from single plant and animal cells. This hybrid source improved the coverage of metabolites of different polarities from 50 metabolites (ESI mode) to 86 metabolites (hybrid mode) in onion cells, and from 40 metabolites (ESI mode) to 111 metabolites (hybrid mode) in PANC-1 cells.

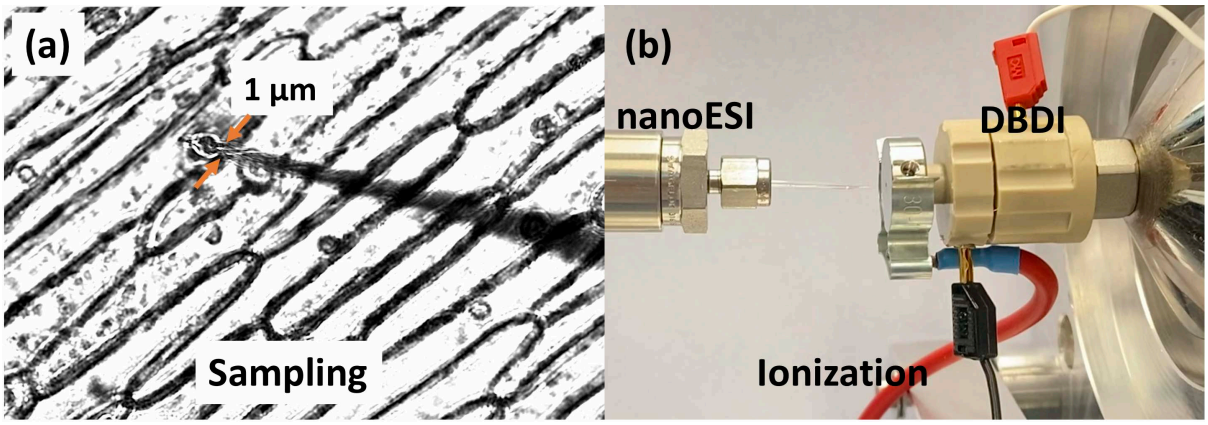

Figure 1. (a) Single cell sampling process. (b) Photo of the nanoESI-DBDI ionization source.

EXPERIMENTAL SECTION

Chemicals

Methanol, acetonitrile, and chlorobenzene were purchased from Sigma-Aldrich Chemie GmbH (Buchs, Switzerland). Testosterone, L-valine, anthracene, fluoranthene, and N,N-dimethylformamide were purchased from Fluka Chemie GmbH (Buchs, Switzerland). L-threonine was purchased from AppliChem GmbH (Darmstadt, Germany). L-cysteine was purchased from abcr GmbH (Karlsruhe, Germany). 08:0 PC and 12:0 PC (DLPC) were purchased from Avanti Polar Lipids (Alabaster, USA). Yellow onions (*Allium cepa*) were

purchased from a local supermarket in Zurich. Phosphate Buffer Saline (PBS) was purchased from Thermo Fisher Scientific (Buchs, Switzerland). PANC-1 cells were purchased from American Type Culture Collection (ATCC).

Sample preparation

Standard solutions of L-threonine, L-valine, L-cysteine, testosterone, 08:0 PC, 12:0 PC (DLPC), anthracene, and fluoranthene were prepared at a concentration of 10 ppm in MeOH/water (1:1), ACN/DMF (1:1), and chlorobenzene/DMF (1:1) separately. A mixture of the eight compounds was prepared at a concentration of 10 ppm in MeOH/water (1:1).

Cell culture and single-cell sampling

The epidermal cell layer of yellow onion bulbs was freshly peeled and placed on a glass slide, which was then placed on the platform of an inverted microscope (Nikon Eclipse Ti Light Microscope). A micropipette puller (Sutter Instrument, Novato, USA) was used to fabricate capillaries with a 1 µm tip. Next, the capillary was inserted into a capillary holder installed on a home-built manipulator. By adjusting the angle and distance between the tip of the capillary and the cell, the capillary was carefully inserted into the cell. The sampling process was observed by optical microscopy (as shown in Figure 1a). Around 30% of the cytoplasmatic cell content was extracted by applying a negative pressure applied by the syringe on the back of the capillary holder. After the cell sampling, the tip of the pulled capillary was backfilled with 2 µL of assistant solvent.

PANC-1 cells were grown in DMEM with 10% (v/v) fetal bovine serum and 1% Penicillin-Streptomycin (P/S) at 37°C in a humidified incubator (Thermo Fisher Scientific) with 5% CO_2. Before single-cell sampling, the dish was washed twice with PBS, then washed twice with

ammonia formate. The dish was then placed on the platform of an inverted microscope to select a target cell and observe the sampling process. The subsequent single PANC-1 cell sampling method was the same as for single onion cells. Sampling images of PANC-1 cell and onion cell are shown in Figure S1.

Hybrid ionization source

In this study, a hybrid ionization source (Figure 1b and S2) that combines nanoESI and DBDI was used to do single-cell analysis. A home-built nanoESI source was used to ionize polar metabolites in cells, followed by an active capillary plasma ionization source (based on a dielectric barrier discharge ionization) to ionize non-polar metabolites in cells. The details about the home-built DBDI source can be found in a previous publication.[27] In brief, the DBDI has two electrodes (Figure S2), an inner electrode (grounded, stainless steel, ID: 0.6 mm and OD: 1.0 mm) and an outer electrode (high voltage, copper, ID: 1.55 mm, around a glass capillary). They are isolated by a glass capillary that acts as a dielectric barrier. When a high AC voltage is applied to the outer electrode, a plasma is ignited inside the capillary. The ignition voltage of DBDI is around 2.0 kVpp. The operating AC voltage of DBDI in this work was 2.2-3.2 kVpp. The DBDI source was connected directly to the inlet capillary of the mass spectrometer to achieve almost 100 % transmission efficiency of the ions formed.

Mass spectrometry

An LTQ Orbitrap mass spectrometer (Thermo Fischer Scientific, San Jose, U.S.A.) was used to acquire mass spectra in positive ion mode, in full-scan mode at a resolution of 30,000 FWHM (at m/z 400) with a mass tolerance specified to be < 10 ppm. The mass-to-charge range was set to 50–1000, capillary voltage was 50 V, tube lens voltage was 120 V, capillary temperature

was 320°C, AGC target = 10^6. Mass spectra were acquired using 1 microscan and a maximum injection time of 50 ms.

Data analysis

The Xcalibur™ software version 2.2 (Thermo Fisher Scientific, San Jose, U.S.A.) was used to record the MS raw data generated from the LTQ orbitrap. MS raw data (.raw) was converted to mzXML format by the MSConvert software (ProteoWizard, v3.0),[40] then imported into Matlab (R2019b version, MathWorks, Natick, MA) for preprocessing.

Metabolite assignments were carried out by comparing the observed mass with the theoretical mass in an onion metabolite database[1] and some other online databases, including Plant Metabolome Database (http://scbt.sastra.edu/pmdb/), Human Metabolome Database (https://hmdb.ca/) and the METLIN metabolite database (https://metlin.scripps.edu/).

RESULTS AND DISCUSSION

Effect of the DBDI source voltage and the nanoESI-DBDI ionization mechanism.

In order to evaluate the ability of nanoESI-DBDI-MS to analyze polar and non-polar compounds, 8 model compounds with different polarities were selected: L-threonine, L-valine, L-cysteine, testosterone, 08:0 PC, 12:0 PC (DLPC), anthracene, and fluoranthene.

We first investigated the effect of the DBDI operating voltage on the ionization efficiency of two compounds with different polarities. During the entire experiment, the nanoESI was turned on, using a voltage of 3.5 kV. As shown in Figure 2a, when the DBDI was turned off, L-threonine was ionized by the ESI source through proton transfer. When the voltage of DBDI was between 2.2-2.8 kV, the signal of L-threonine was higher than with only the ESI running.

This may be because reactive species in the plasma (H^+, H_3O^+, cluster ions, etc.) can increase the overall ion yield of L-threonine via proton transfer. However, the signal of L-threonine decreased with increasing DBDI voltage. Above 2.8 kV, the signal of L-threonine dropped significately. We interpret this to be the result of L-threonine fragmentation (Figure S3), resulting in a decrease in its parent ion signal. On the contrary, anthracene could not be ionized when only the ESI was turned on (Figure 2b). When the DBDI was turned on, the signal of anthracene increased with increasing DBDI voltage. Anthracene may thus be mainly ionized via charge transfer, electron impact, or Penning ionization. As the DBDI voltage increases, the number of electrons in the plasma also increases, which helps to ionize anthracene, resulting in a signal enhancement. When the voltage of the DBDI source was 2.6 kV, the intensity of L-threonine was higher than when only the ESI was turned on, and the signal of anthracene was also relatively stable. Therefore, 2.6 kV was selected as the DBDI operating voltage for subsequent experiments.

In general, by simply adjusting the DBDI voltage from low to high (0-3.2 kV), the ionization reaction in the hybrid nanoESI-DBDI source is switched from proton transfer to charge transfer, electron impact, and Penning ionization. In this way, nanoESI-DBDI-MS can detect not only polar compounds but also analyze non-polar compounds.

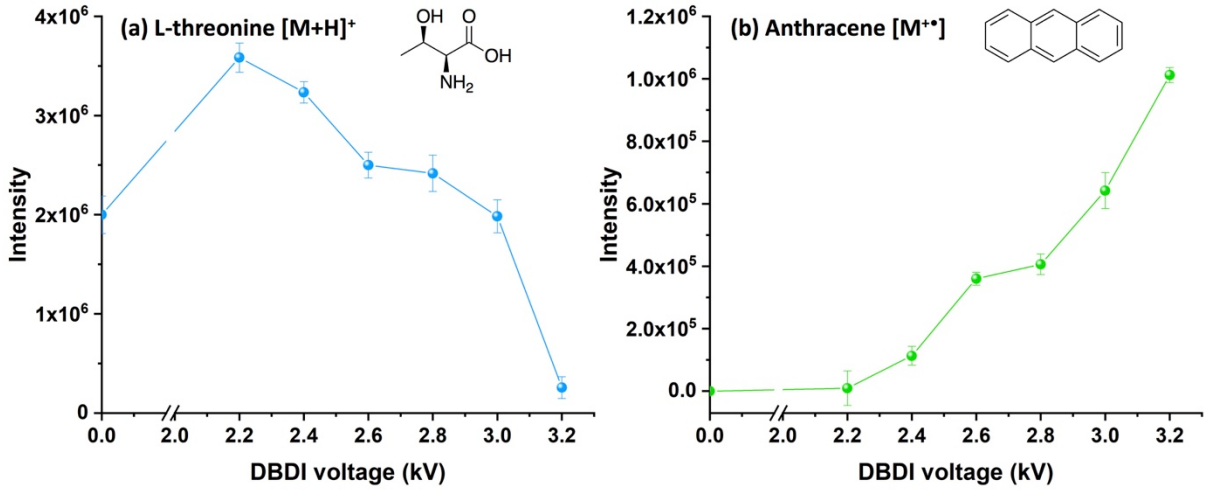

Figure 2. Effect of the DBDI voltage on the intensity of (a) L-threonine and (b) anthracene. ESI voltage was set to 3.5 kV in both cases.

Effect of assistant solvents

The effect of different solvents on the ionization efficiency of the model compounds was also studied.[34,41] Three solvent mixtures with different polarities (MeOH: water=1:1, ACN: DMF=1:1, chlorobenzene: DMF=1:1) were used to dissolve the samples investigated here. The effect of these three assistant solvents on the intensity of the 8 model compounds are shown in Figure S4 and described in full detail in section 3 of the supporting information (SI). Since both polar compounds and non-polar compounds have good ionization efficiencies when MeOH/water (1:1) was used as the assistant solvent, MeOH/water (1:1) was selected as the solvent for subsequent experiments.

The mass spectra of the 8 compounds dissolved in MeOH/water(1:1) are shown in Figure 3. In ESI mode, the product ions of 3 polar amino acids appeared as $[M+H]^+$ (Figure 3a, b, and c). In hybrid mode, the ionization efficiencies of all product ions increased. For the three lipids (Figure 3d, e, and f), the observed product ions were $[M+H]^+$ and $[M+Na]^+$. Turning on the DBDI increased the ionization efficiencies of all product ions. For the two non-polar PAHs (Figure 3g and h), no prominent product ions were observed in ESI only mode. In hybrid mode, $[M]^{+\bullet}$ ions were the dominant product ions. Based on the above results, it can be seen that when the DBDI voltage was set to 2.6 kV, the protonated species (RH^+) in the plasma could improve the ionization of polar compounds to produce protonated molecular ions. Moreover, radical cations in the plasma could also promote ionization of nonpolar compounds.

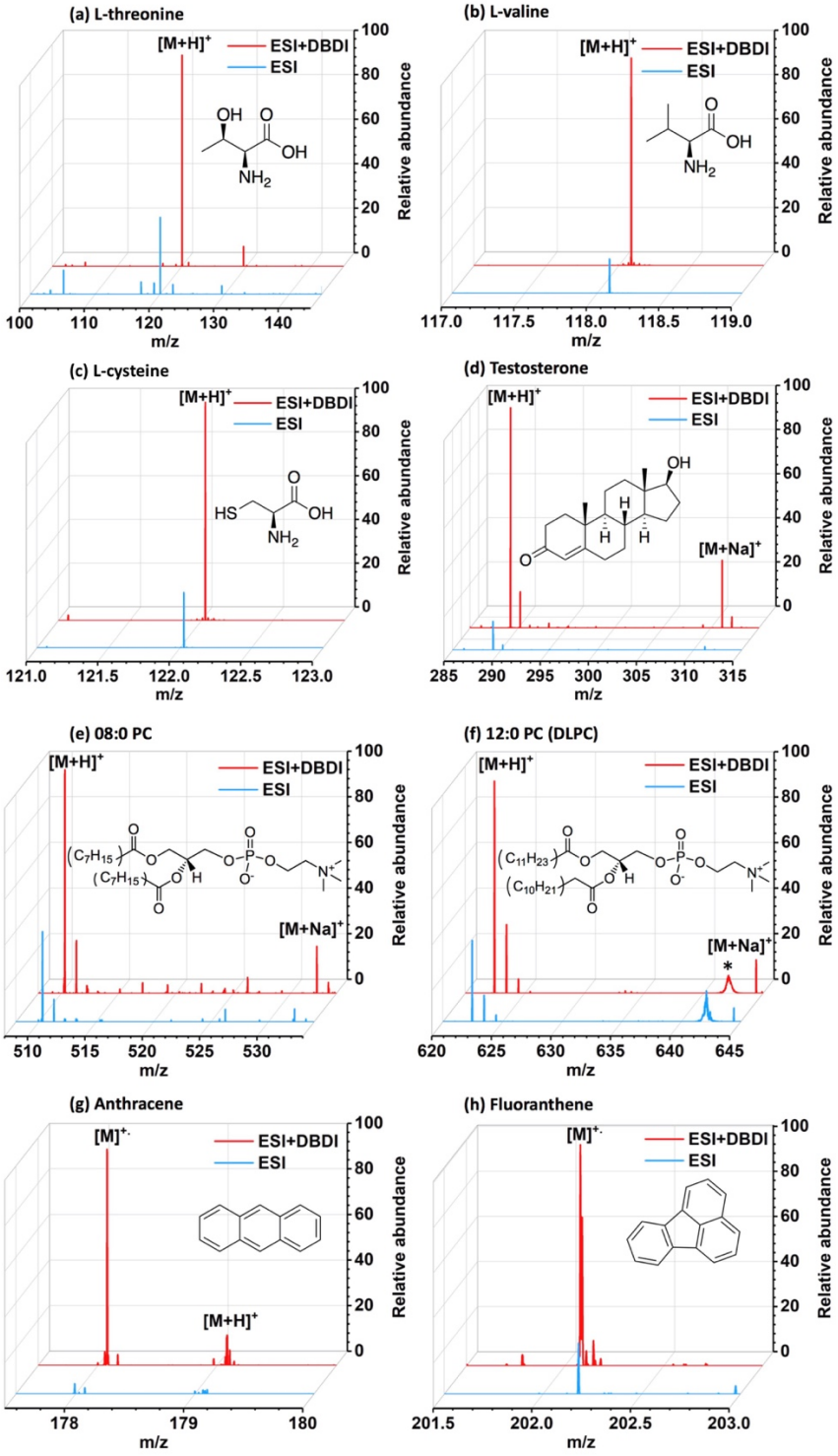

Figure 3. Mass spectra of 8 model compounds with different polarities ionized by ESI and ESI-DBDI (solvent MeOH: water=1:1). (a) L-threonine, (b) L-valine, (c) L-cysteine, (d) testosterone, (e) 08:0 PC, (f) 12:0 PC (DLPC), (g) anthracene and (h) fluoranthene. (ESI voltage: 3.5 kV; DBDI voltage: 2.6 kV; the asterisk (*) indicates electronic noise in the spectra.)

By analyzing a mixture containing 8 polar and non-polar compounds, the ability of the hybrid source to simultaneously detect mixtures was further evaluated. As shown in Figure 4, L-threonine, L-valine, L-cysteine, testosterone, 08:0 PC, and 12:0 PC (DLPC) could be ionized in ESI mode, and their product ions were $[M+H]^+$. No product ions from anthracene and fluoranthene were observed. In the "ESI+DBDI" mode, L-threonine, L-valine, L-cysteine, testosterone, 08:0 PC, 12:0 PC (DLPC), and anthracene were all detected. The product ion of anthracene was $[M]^{+\bullet}$, the product ions of other compounds were also $[M+H]^+$, and the intensity of all the product ions was significantly improved except for fluoranthene. Although no product ions from fluoranthene were observed in the mixture due to the ion suppression effects among different product ions, fluoranthene can be ionized by ESI-DBDI alone. The signal-to-noise ratios (S/N) of the 8 model compounds indeed improved after turning on the DBDI. For example, the S/N of L-threonine increased ~3 times.

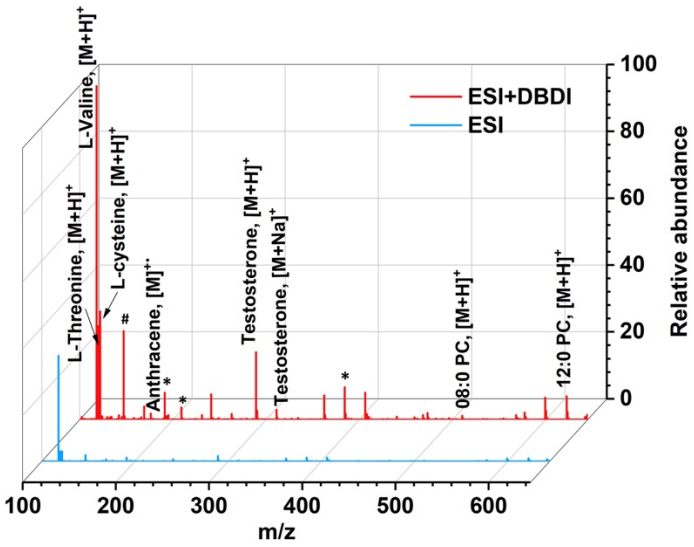

Figure 4. mass spectrum of a mixture of eight model compounds with different polarities, L-threonine, L-valine, L-cysteine, testosterone, 08:0 PC, 12:0 PC (DLPC), anthracene, and

fluoranthene. (ESI voltage: 3.5 kV; DBDI voltage: 2.6 kV; the pound sign ($^{\#}$) indicates ACN + MeOH clusters; the asterisk (*) indicates electronic noise in the spectra.)

Single-cell metabolite analysis

We then applied the ESI-DBDI hybrid source to analyze metabolites in both single plant cells and animal cells, analyzing dozens of cells and measuring at least 3 replicates for each cell type to validate the reproducibility and robustness of our method. We first chose onion cells as an application example, because single-cell analysis of onion cells has been widely reported.[1,20,42,43] It is also relatively easy to do sampling on an onion cell. After microsampling, the onion cell metabolites were analyzed by ESI-DBDI-MS. In positive ion mode (m/z range between 50-1000), approximately 50 metabolites were detected in ESI mode in onion cells (Table S1). The observed product ions were mostly $[M+H]^+$ and $[M+Na]^+$, which are commonly seen in ESI. Some other common in-source fragments like $[M+H-H_2O]^+$ and $[M+H-2H_2O]^+$ were also observed.[44] When the DBDI was turned on (2.6-2.8 kV), approximately 86 metabolites were detected (Table S2), among them 49 metabolites that were not observed in ESI only mode. Most of them were non-polar. Except for $[M+H]^+$, $[M+Na]^+$, $[M+H-H_2O]^+$ and $[M+H-2H_2O]^+$, $[M]^{+\bullet}$ ions were also formed in hybrid mode.

Among all ionized metabolites in the onion cell, three polar metabolites (threonine, glutamine, and serine) and three non-polar metabolites (2,5-dimethylthiophene, 1-propenyl propyl disulfide, and 5-hydroxymethyl-2-furancarboxaldehyde) were chosen as markers to highlight the differences between the ESI mode and the hybrid mode in detail. As shown in Figure 5a, when only ESI was on, only polar metabolites (threonine, glutamine, and serine) were detected. When the DBDI voltage was between 2.2 kV to 2.4 kV, the signal of threonine did not change significantly, and the signals of glutamine and serine were slightly reduced. At

the same time, less polar metabolites (2,5-dimethylthiophene and 1-propenyl propyl disulfide) could be observed, but no clear signal from 5-hydroxymethyl-2-furancarboxaldehyde was observed. When the DBDI voltage was between 2.6 kV to 2.8 kV, the signal of polar metabolites (threonine, glutamine, and serine) decreased somewhat, while the signals of less polar metabolites (2,5-dimethylthiophene, 1-propenyl propyl disulfide, and 5-hydroxymethyl-2-furancarboxaldehyde) increased significantly. When the DBDI voltage was between 3 kV to 3.2 kV, the signal of polar compounds was significantly reduced. Especially for glutamine, almost no obvious signal remained, but the signal of non-polar compounds was further improved. By comparing the mass spectra of an onion cell in ESI mode (Figure 5b) and in hybrid mode (Figure 5c), it can be seen that the mass spectral profiles are quite different. For example, in ESI mode (Figure 6a), abundant peaks were at m/z 102.06 (assigned to threonine), m/z 164.07 (S-propyl-L-cysteine), m/z 175.12 (arginine), m/z 184.07 (phosphorylcholine), which are polar onion cell metabolites. When the DBDI voltage was switched on to 2.6 kV (Figure 6b), less polar metabolites such as 3-(methylthiomethylthio)-1-propene (m/z 89.04), 2,5-dimethylthiophene (m/z 113.04) and di-1-propenyl sulfide (m/z 115.05) were also observed in addition to polar metabolites such as furfuryl acetate (m/z 123.04), arginine (m/z 175.12) and citrullin (m/z 198.09).

We also invistigated PANC-1 cells, as an example of a human cell, by ESI-DBDI-MS in this study. As shown in Table S3, there were around 40 metabolites observed in ESI mode. The observed product ions and in-source fragments included $[M+H]^+$, $[M+Na]^+$, $[M+K]^+$, $[M+H-H_2O]^+$ and $[M+H-2H_2O]^+$. Approximately 111 metabolites were detected (Table S4) in a single PANC-1 cell when the DBDI was turned on (2.6-2.8 kV), of which additional 71 metabolites were not observed in ESI only mode. $[M+H]^+$, $[M+Na]^+$, $[M+K]^+$, $[M+H-H_2O]^+$, $[M]^{+\bullet}$ ions were the observed product ions in hybrid mode.

Three polar (leucine, lysine, and arginine) and three non-polar metabolites (1-pyrroline, dimethylurea, and a-methylstyrene) were selected as markers from all the ionized compounds to show the difference between ESI mode and hybrid mode. As shown in Figure 6a, non-polar metabolites (1-pyrroline, dimethylurea, and a-methylstyrene) were not detectable in ESI only mode. When the DBDI voltage was between 2.2 kV to 2.6 kV, non-polar metabolites (1-pyrroline, dimethylurea, and a-methylstyrene) were observed. At the same time, the signal of polar metabolites (leucine, lysine, and arginine) significantly increased. When the DBDI voltage was between 2.8 kV to 2.3 kV, the signal of polar metabolites (leucine, lysine, and arginine) was reduced, while the signals of non-polar metabolites (1-pyrroline, dimethylurea, and a-methylstyrene) increased slightly. When the DBDI voltage was 3.2 kV, the signals of polar compounds were almost non-detectable, while the signals of non-polar compounds did not change obviously. The mass spectral profiles of a PANC-1 cell in ESI mode and hybrid mode are evidently different. In ESI mode (Figure 6b), abundant peaks were at m/z 116.07 (assigned to proline), m/z 132.08 (creatine), m/z 147.11 (lysine), m/z 154.08 (leucine), which are polar PANC-1 cell metabolites. When the DBDI voltage was switched on to 2.6 kV (Figure 6b), polar metabolites including 1-pyrroline (m/z 70.06), pyridine (m/z 80.05) and so on, and non-polar metabolites including proline (m/z 116.07), threonine (m/z 142.05), etc. were detected at the same time.

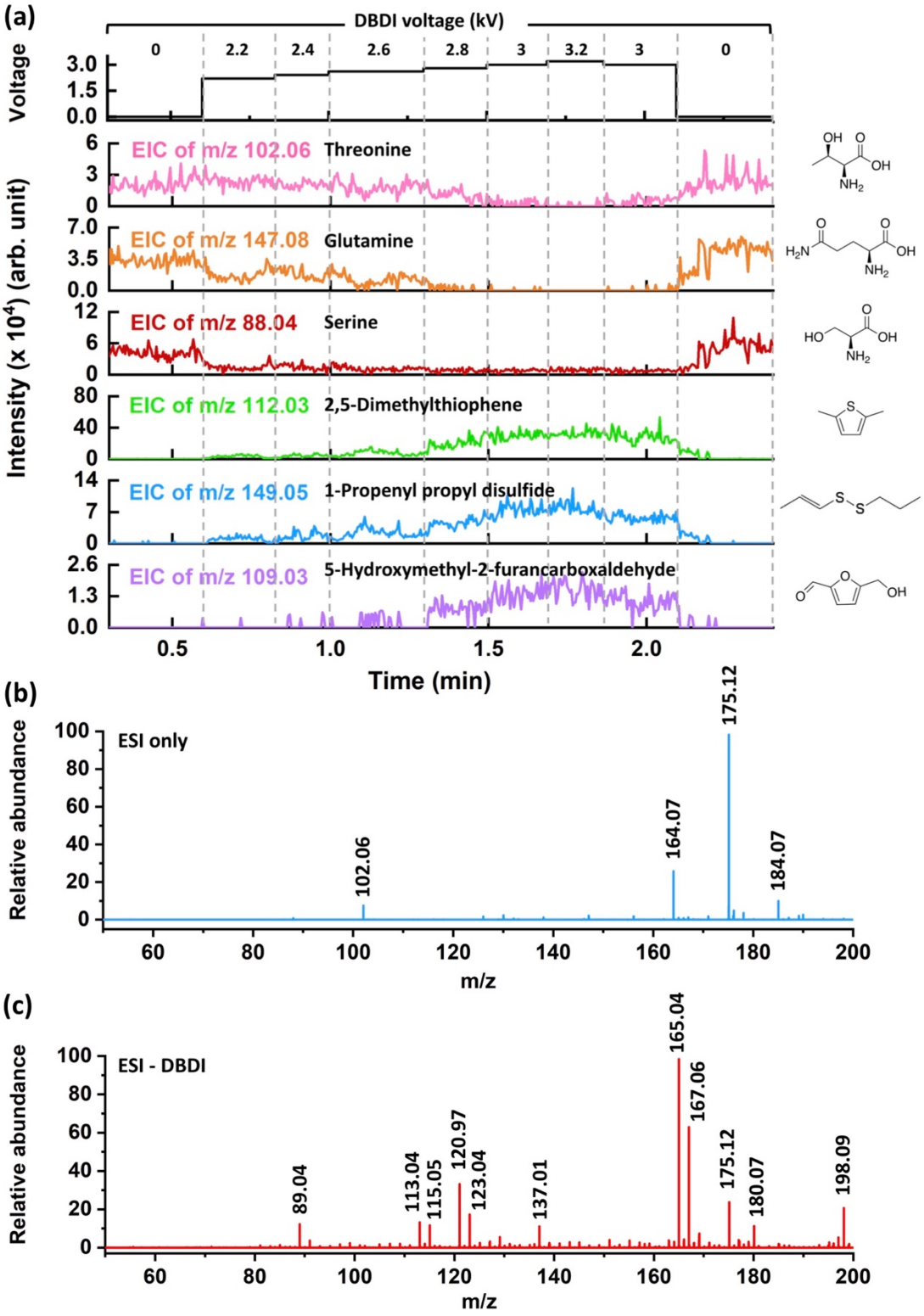

Figure 5. Metabolite analysis in a representative single onion cell. (a) total ion chromatogram (TIC) and extracted ion chromatograms (EICs) of six metabolites in onion cells in ESI/hybrid mode. (ESI was always on: 3.5 kV), (b) mass spectrum acquired in ESI (3.5 kV) mode, (c) mass spectrum acquired in ESI (3.5 kV)-DBDI (2.6 kV) hybrid mode.

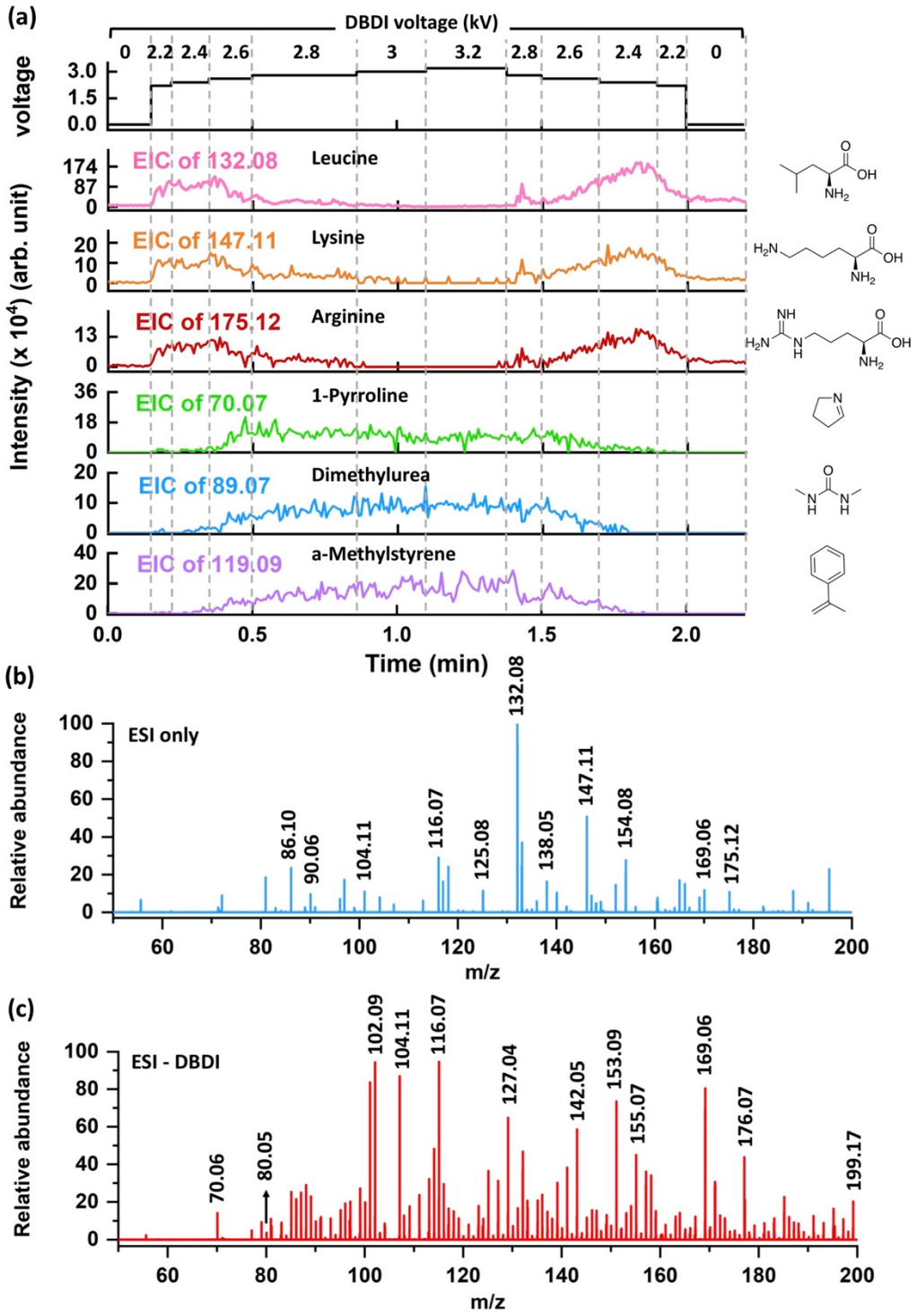

Figure 6. Metabolite analysis in a representative single PANC-1 cell. (a) total ion chromatogram (TIC) and extracted ion chromatograms (EICs) of six metabolites in onion cells in ESI/hybrid mode. (ESI was always on: 3.5 kV, A: DBDI off, B: DBDI 2.2 kV, C: DBDI 2.4 kV, D: DBDI 2.6 kV, E: DBDI 2.8 kV, F: DBDI 3 kV, G: DBDI 3.2 kV), (b) mass spectrum acquired in ESI (3.5 kV) mode, (c) mass spectrum acquired in ESI (3.5 kV)-DBDI (2.6 kV) hybrid mode.

The above results further confirmed that by adjusting the DBDI voltage, the ESI-DBDI source can be switched to different modes. When the DBDI is turned off, the metabolites in the cells are mainly ionized by the ESI source through proton transfer. Due to the complex environment in the cells, matrix effects, and ion suppression, the ion yield of less polar and non-polar metabolites is reduced. Since DBDI is less affected by matrix effects and ion suppression effect than ESI, and there are many reactive species in the plasma, turning on the DBDI increased the ion yield of less polar and non-polar metabolites via a range of ionization reactions, including proton transfer, charge transfer, electron impact and Penning ionization. For high-throughput single-cell analysis, on-line infusion of a cell suspension into the hybrid source presented here could be used [35], and an automatic voltage scan, similar to data independent acquisition in LC-MS, could be helpful.

CONCLUSIONS

In this study, a hybrid ESI+DBDI ionization source was developed for single-cell analysis. The ESI-DBDI source can be operated in ESI mode and hybrid mode. In ESI mode, polar metabolites are ionized well. In hybrid mode, non-polar or less non-polar metabolites exhibit good ionization efficiency. By gradually increasing the DBDI voltage from 0 to 3.2 kV, the classes of ionized metabolites in cells can be shifted from mostly polar, to both polar and apolar, to mainly apolar. This hybrid ESI+DBDI source apparently relies on multiple ionization mechanisms such as proton transfer, charge transfer, and Penning ionization. It can thereby improve the ionization efficiency of metabolites of different polarities, the limit if detection, and the coverage of metabolites, which may contribute to the development of metabolomics at the single-cell level.

ASSOCIATED CONTENT

Supporting Information

Single-cell sampling images, fragment ions mass spectrum of L-threonine, effect of assistant solvents, and metabolites from single cell ionized by ESI source and hybrid source. (PDF)

AUTHOR INFORMATION

Corresponding Author

Renato Zenobi − *Department of Chemistry and Applied Biosciences, ETH Zurich, Zurich CH-8093, Switzerland; orcid.org/0000-0001-5211-4358; Phone: +41 44 632 43 76; Email: zenobi@org.chem.ethz.ch; Fax: +41 44 632 292*

Authors

Qinlei Liu − *Department of Chemistry and Applied Biosciences, ETH Zurich, Zurich CH-8093, Switzerland*

Jiayi Lan − *Department of Chemistry and Applied Biosciences, ETH Zurich, Zurich CH-8093, Switzerland*

Ri Wu − *Department of Chemistry and Applied Biosciences, ETH Zurich, Zurich CH-8093, Switzerland*

Alina Begley − *Department of Chemistry and Applied Biosciences, ETH Zurich, Zurich CH-8093, Switzerland*

Wenjie Ge − *Department of Biology, ETH Zurich, CH-8093 Zurich, Switzerland*

Notes

The authors declare no competing financial interest.

The original data used in this publication have been made available in a curated data archive at ETH Zurich (https://www.researchcollection.ethz.ch) under the DOI: 10.3929/ethz-b-000506474.

ACKNOWLEDGMENTS

Qinlei Liu thanks the China Scholarship Council (CSC) for financial support of her Ph.D. research (Grant Number: 201906240053). We thank all members of the Zenobi group, especially Dr. Sandra Martínez-Jarquín for helpful discussion and suggestions.

TOC

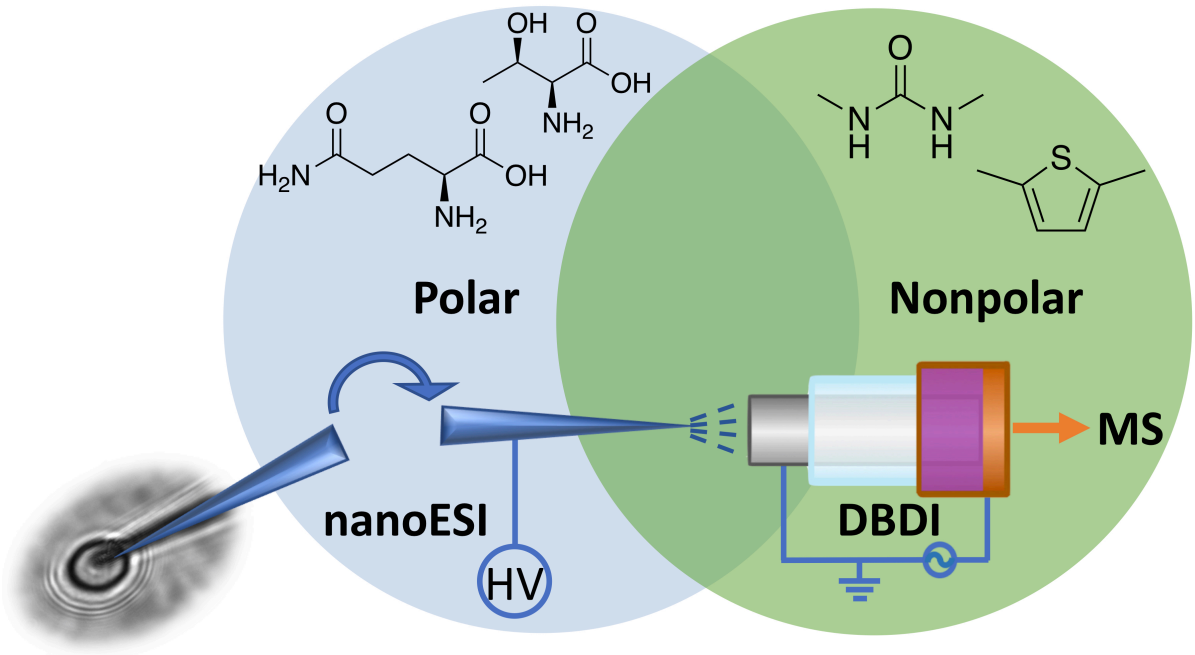

REFERENCES

(1) Huang, L.; Fang, M.; Cupp-Sutton, K. A.; Wang, Z.; Smith, K.; Wu, S. Spray-Capillary-Based Capillary Electrophoresis Mass Spectrometry for Metabolite Analysis in Single Cells. *Anal. Chem.* **2021**, *93*, 4479-4487.

(2) Li, Z.; Wang, Z.; Pan, J.; Ma, X.; Zhang, W.; Ouyang, Z. Single-Cell Mass Spectrometry Analysis of Metabolites Facilitated by Cell Electro-Migration and Electroporation. *Anal. Chem.* **2020**, *92*, 10138-10144.

(3) Yuan, Z.; Zhou, Q.; Cai, L.; Pan, L.; Sun, W.; Qumu, S.; Yu, S.; Feng, J.; Zhao, H.; Zheng, Y.; Shi, M.; Li, S.; Chen, Y.; Zhang, X.; Zhang, M. Q. SEAM is a Spatial Single Nuclear Metabolomics Method for Dissecting Tissue Microenvironment. *Nat. Methods* **2021**, *18*, 1223-1232.

(4) Li, Z.; Cheng, S.; Lin, Q.; Cao, W.; Yang, J.; Zhang, M.; Shen, A.; Zhang, W.; Xia, Y.; Ma, X.; Ouyang, Z. Single-cell Lipidomics with High Structural Specificity by Mass Spectrometry. *Nat. Commun.* **2021**, *12*, 2869.

(5) Liu, F. L.; Ye, T. T.; Ding, J. H.; Yin, X. M.; Yang, X. K.; Huang, W. H.; Yuan, B. F.; Feng, Y. Q. Chemical Tagging Assisted Mass Spectrometry Analysis Enables Sensitive Determination of Phosphorylated Compounds in a Single Cell. *Anal. Chem.* **2021**, *93*, 6848-6856.

(6) Neumann, E. K.; Ellis, J. F.; Triplett, A. E.; Rubakhin, S. S.; Sweedler, J. V. Lipid Analysis of 30000 Individual Rodent Cerebellar Cells Using High-Resolution Mass Spectrometry. *Anal. Chem.* **2019**, *91*, 7871-7878.

(7) Do, T. D.; Comi, T. J.; Dunham, S. J.; Rubakhin, S. S.; Sweedler, J. V. Single Cell Profiling Using Ionic Liquid Matrix-Enhanced Secondary Ion Mass Spectrometry for Neuronal Cell Type Differentiation. *Anal. Chem.* **2017**, *89*, 3078-3086.

(8) Lanni, E. J.; Dunham, S. J.; Nemes, P.; Rubakhin, S. S.; Sweedler, J. V. Biomolecular Imaging with a C60-SIMS/MALDI Dual Ion Source Hybrid Mass Spectrometer: Instrumentation, Matrix Enhancement, and Single Cell Analysis. *J. Am. Soc. Mass Spectrom.* **2014**, *25*, 1897-1907.

(9) Neumann, E. K.; Comi, T. J.; Rubakhin, S. S.; Sweedler, J. V. Lipid Heterogeneity between Astrocytes and Neurons Revealed by Single-Cell MALDI-MS Combined with Immunocytochemical Classification. *Angew. Chem., Int. Ed. Engl.* **2019**, *58*, 5910-5914.

(10) Amantonico, A.; Oh, J. Y.; Sobek, J.; Heinemann, M.; Zenobi, R. Mass Spectrometric Method for Analyzing Metabolites in Yeast with Single Cell Sensitivity. *Angew. Chem., Int. Ed. Engl.* **2008**, *47*, 5382-5385.

(11) Zhuang, M.; Hou, Z.; Chen, P.; Liang, G.; Huang, G. Introducing Charge Tag via Click Reaction in Living Cells for Single cell Mass Spectrometry. *Chem. Sci.* **2020**, *11*, 7308-7312.

(12) Kompauer, M.; Heiles, S.; Spengler, B. Atmospheric Pressure MALDI Mass Spectrometry Imaging of Tissues and Cells at 1.4-mum Lateral Resolution. *Nat. Methods* **2017**, *14*, 90-96.

(13) Tian, H.; Sparvero, L. J.; Blenkinsopp, P.; Amoscato, A. A.; Watkins, S. C.; Bayir, H.; Kagan, V. E.; Winograd, N. Secondary-Ion Mass Spectrometry Images Cardiolipins and Phosphatidylethanolamines at the Subcellular Level. *Angew. Chem., Int. Ed. Engl.* **2019**, *58*, 3156-3161.

(14) Abouleila, Y.; Onidani, K.; Ali, A.; Shoji, H.; Kawai, T.; Lim, C. T.; Kumar, V.; Okaya, S.; Kato, K.; Hiyama, E.; Yanagida, T.; Masujima, T.; Shimizu, Y.; Honda, K. Live Single Cell Mass Spectrometry Reveals Cancer-Specific Metabolic Profiles of Circulating Tumor Cells. *Cancer Sci.* **2019**, *110*, 697-706.

(15) Fujii, T.; Matsuda, S.; Tejedor, M. L.; Esaki, T.; Sakane, I.; Mizuno, H.; Tsuyama, N.; Masujima, T. Direct Metabolomics for Plant Cells by Live Single-Cell Mass Spectrometry. *Nat. Protoc.* **2015**, *10*, 1445-1456.

(16) Tsuyama, N.; Mizuno, H.; Tokunaga, E.; Masujima, T. Live Single-Cell Molecular Analysis by Video-Mass Spectrometry. *Anal. Sci.* **2008**, *24*, 559-561.

(17) Zhang, L.; Foreman, D. P.; Grant, P. A.; Shrestha, B.; Moody, S. A.; Villiers, F.; Kwak, J. M.; Vertes, A. In Situ Metabolic Analysis of Single Plant Cells by Capillary Microsampling and Electrospray Ionization Mass Spectrometry with Ion Mobility Separation. *Analyst* **2014**, *139*, 5079-5085.

(18) Zhang, L.; Khattar, N.; Kemenes, I.; Kemenes, G.; Zrinyi, Z.; Pirger, Z.; Vertes, A. Subcellular Peptide Localization in Single Identified Neurons by Capillary Microsampling Mass Spectrometry. *Sci. Rep.* **2018**, *8*, 12227.

(19) Zhang, L.; Vertes, A. Energy Charge, Redox State, and Metabolite Turnover in Single Human Hepatocytes Revealed by Capillary Microsampling Mass Spectrometry. *Anal. Chem.* **2015**, *87*, 10397-10405.

(20) Shrestha, B.; Vertes, A. In Situ Metabolic Profiling of Single Cells by Laser Ablation Electrospray Ionization Mass Spectrometry. *Anal. Chem.* **2009**, *81*, 8265-8271.

(21) Stolee, J. A.; Vertes, A. Toward Single-Cell Analysis by Plume Collimation in Laser Ablation Electrospray Ionization Mass Spectrometry. *Anal. Chem.* **2013**, *85*, 3592-3598.

(22) Stopka, S. A.; Wood, E. A.; Khattar, R.; Agtuca, B. J.; Abdelmoula, W. M.; Agar, N. Y. R.; Stacey, G.; Vertes, A. High-Throughput Analysis of Tissue-Embedded Single Cells by Mass Spectrometry with Bimodal Imaging and Object Recognition. *Anal. Chem.* **2021**, *93*, 9677-9687.

(23) Lombard-Banek, C.; Moody, S. A.; Manzini, M. C.; Nemes, P. Microsampling Capillary Electrophoresis Mass Spectrometry Enables Single-Cell Proteomics in Complex Tissues: Developing Cell Clones in Live Xenopus laevis and Zebrafish Embryos. *Anal. Chem.* **2019**, *91*, 4797-4805.

(24) Lombard-Banek, C.; Moody, S. A.; Nemes, P. Single-Cell Mass Spectrometry for Discovery Proteomics: Quantifying Translational Cell Heterogeneity in the 16-Cell Frog (Xenopus) Embryo. *Angew. Chem., Int. Ed. Engl.* **2016**, *55*, 2454-2458.

(25) Onjiko, R. M.; Moody, S. A.; Nemes, P. Single-cell Mass Spectrometry Reveals Small Molecules that Affect Cell Fates in the 16-cell Embryo. *Proc. Natl. Acad. Sci. U. S. A.* **2015**, *112*, 6545-6550.

(26) Lombard-Banek, C.; Li, J.; Portero, E. P.; Onjiko, R. M.; Singer, C. D.; Plotnick, D. O.; Al Shabeeb, R. Q.; Nemes, P. In Vivo Subcellular Mass Spectrometry Enables Proteo-Metabolomic Single-Cell Systems Biology in a Chordate Embryo Developing to a Normally Behaving Tadpole (X. laevis)*. *Angew. Chem., Int. Ed. Engl.* **2021**, *60*, 12852-12858.

(27) Liu, Q.; Zenobi, R. Rapid Analysis of Fragrance Allergens by Dielectric Barrier Discharge Ionization Mass Spectrometry. *Rapid Commun. Mass Spectrom.* **2020**, e9021.

(28) Gyr, L.; Klute, F. D.; Franzke, J.; Zenobi, R. Characterization of a Nitrogen-Based Dielectric Barrier Discharge Ionization Source for Mass Spectrometry Reveals Factors Important for Soft Ionization. *Anal. Chem.* **2019**, *91*, 6865-6871.

(29) Adamovich, I.; Baalrud, S. D.; Bogaerts, A.; Bruggeman, P. J.; Cappelli, M.; Colombo, V.; Czarnetzki, U.; Ebert, U.; Eden, J. G.; Favia, P.; Graves, D. B.; Hamaguchi, S.; Hieftje, G.; Hori, M.; Kaganovich, I. D.; Kortshagen, U.; Kushner, M. J.; Mason, N. J.; Mazouffre, S.; Thagard, S. M., et al. The 2017 Plasma Roadmap: Low Temperature Plasma Science and Technology. *J. Phys. D: Appl. Phys.* **2017**, *50*.

(30) Brandt, S.; Klute, F. D.; Schutz, A.; Franzke, J. Dielectric Barrier Discharges Applied for Soft Ionization and Their Mechanism. *Anal. Chim. Acta* **2017**, *951*, 16-31.

(31) Wolf, J. C.; Gyr, L.; Mirabelli, M. F.; Schaer, M.; Siegenthaler, P.; Zenobi, R. A Radical-Mediated Pathway for the Formation of [M + H](+) in Dielectric Barrier Discharge Ionization. *J. Am. Soc. Mass Spectrom.* **2016**, *27*, 1468-1475.

(32) Gyr, L.; Wolf, J. C.; Franzke, J.; Zenobi, R. Mechanistic Understanding Leads to Increased Ionization Efficiency and Selectivity in Dielectric Barrier Discharge Ionization Mass Spectrometry: A Case Study with Perfluorinated Compounds. *Anal. Chem.* **2018**, *90*, 2725-2731.

(33) Müller, S.; Krähling, T.; Veza, D.; Horvatic, V.; Vadla, C.; Franzke, J. Operation Modes of the Helium Dielectric Barrier Discharge for Soft Ionization. *Spectrochim. Acta, Part B* **2013**, *85*, 104-111.

(34) Huba, A. K.; Mirabelli, M. F.; Zenobi, R. High-throughput Screening of PAHs and Polar Trace Contaminants in Water Matrices by Direct Solid-Phase Microextraction Coupled to a Dielectric Barrier Discharge Ionization Source. *Anal. Chim. Acta* **2018**, *1030*, 125-132.

(35) Liu, Q.; Ge, W.; Wang, T.; Lan, J.; Martinez-Jarquin, S.; Wolfrum, C.; Stoffel, M.; Zenobi, R. High-throughput Single-cell Mass Spectrometry Reveals Abnormal Lipid Metabolism in Pancreatic Ductal Adenocarcinoma. *Angew Chem Int Ed Engl* **2021**, *60*, 24534-23542.

(36) Cheng, S. C.; Jhang, S. S.; Huang, M. Z.; Shiea, J. Simultaneous Detection of Polar and Nonpolar Compounds by Ambient Mass Spectrometry with a Dual Electrospray and Atmospheric Pressure Chemical Ionization Source. *Anal. Chem.* **2015**, *87*, 1743-1748.

(37) Barry, J. A.; Robichaud, G.; Bokhart, M. T.; Thompson, C.; Sykes, C.; Kashuba, A. D.; Muddiman, D. C. Mapping Antiretroviral Drugs in Tissue by IR-MALDESI MSI Coupled to the Q Exactive and Comparison with LC-MS/MS SRM Assay. *J. Am. Soc. Mass Spectrom.* **2014**, *25*, 2038-2047.

(38) Rosen, E. P.; Bokhart, M. T.; Ghashghaei, H. T.; Muddiman, D. C. Influence of Desorption Conditions on Analyte Sensitivity and Internal Energy in Discrete Tissue or Whole Body Imaging by IR-MALDESI. *J. Am. Soc. Mass Spectrom.* **2015**, *26*, 899-910.

(39) Stark, A. K.; Meyer, C.; Kraehling, T.; Jestel, G.; Marggraf, U.; Schilling, M.; Janasek, D.; Franzke, J. Electronic Coupling and Scaling Effects During Dielectric Barrier Electrospray Ionization. *Anal. Bioanal. Chem.* **2011**, *400*, 561-569.

(40) Adusumilli, R.; Mallick, P. Data Conversion with ProteoWizard msConvert. In *Proteomics: Methods and Protocols*, Comai, L.; Katz, J. E.; Mallick, P., Eds.; Springer New York: New York, NY, 2017, pp 339-368.

(41) Huba, A. K.; Mirabelli, M. F.; Zenobi, R. Understanding and Optimizing the Ionization of Polycyclic Aromatic Hydrocarbons in Dielectric Barrier Discharge Sources. *Anal. Chem.* **2019**, *91*, 10694-10701.

(42) Yin, R.; Prabhakaran, V.; Laskin, J. Quantitative Extraction and Mass Spectrometry Analysis at a Single-Cell Level. *Anal. Chem.* **2018**, *90*, 7937-7945.

(43) Gong, X.; Zhao, Y.; Cai, S.; Fu, S.; Yang, C.; Zhang, S.; Zhang, X. Single Cell Analysis with Probe ESI-Mass Spectrometry: Detection of Metabolites at Cellular and Subcellular Levels. *Anal. Chem.* **2014**, *86*, 3809-3816.

(44) Varghese, R. S.; Zhou, B.; Nezami Ranjbar, M. R.; Zhao, Y.; Ressom, H. W. On Annotation-Assisted Analysis of LC-MS based Metabolomic Experiment. *Proteome Sci.* **2012**, *10 Suppl 1*, S8-S8.